







Cite this: *J. Anal. At. Spectrom.*, 2022, **37**, 1618

Ce and Nd stable isotope purification and determination of geological samples by MC-ICP-MS†

Jiang-Hao Bai,  ^{abd} Jin-Long Ma,  ^{*a} Gang-Jian Wei,  ^{ab} Le Zhang  ^a and Song-Xiong Zhong^c

The combined study of Ce and Nd stable isotopes is promising because Ce and Nd behave similarly in geological processes and distinctively in redox reactions. However, the sequential purification of Ce and Nd from other REEs is particularly challenging because of their similar physicochemical properties. In this contribution, we present a novel two-stage ion-exchange chromatography method to purify Ce and then Nd using Bio-Rad AG50W-X12 (200–400 mesh) and Eichrom TODGA resin (50–100 μm). The yields of Ce and Nd are both typically more than 99.3% after measurements of natural materials. The potential influence of the HCl content and rock type were thoroughly evaluated. Stable Ce and Nd isotopic ratios were measured by MC-ICPMS and calibrated with Sm and Eu internal standards, respectively. The long-term external reproducibility was better than $\pm 0.04\text{‰}$ (2SD) for $\delta^{142/140}\text{Ce}$ and $\pm 0.03\text{‰}$ (2SD) for $\delta^{146/144}\text{Nd}$. The stable Ce and Nd isotopic ratios of ten commercially accessible geological rocks were measured here. The $\delta^{142/140}\text{Ce}$ values of four geological rocks were presented for the first time. Other results are in good accordance with reported values within analytical uncertainties. The similarity in the degree of Ce and Nd isotopic fractionation may be induced by diagenetic processes, whereas the difference may be accused by redox reactions. In addition, our method using a single sample aliquot can help to minimize the consumptions and heterogeneities of the samples. This procedure for a two-stage isolation of Ce and Nd and high-precision analysis of their isotopic ratios has important advantages in the study of Ce and Nd isotope geochemistry.

Received 7th March 2022
 Accepted 8th June 2022

DOI: 10.1039/d2ja00082b
[rsc.li/jaas](https://doi.org/10.1039/d2ja00082b)

1. Introduction

Cerium (Ce) is a lithophile and refractory rare earth element (REE). It has four natural isotopes, ^{136}Ce (0.185%), ^{138}Ce (0.251%), ^{140}Ce (88.450%) and ^{142}Ce (11.114%).¹ Cerium (Ce) has been studied for isotopic variations in two ways, the ^{138}La – ^{138}Ce decay system ($T_{1/2} = 102 \text{ Ga}$)^{2,3} and Ce stable isotopic system ($\delta^{142/140}\text{Ce}$).⁴ The ^{138}La – ^{138}Ce decay system has been applied to geochronology and as a radiogenic isotope tracer in the Earth and planetary sciences.^{3,5–7} The Ce stable isotopic system ($\delta^{142/140}\text{Ce}$) is in its infancy. Nakada *et al.*⁴ first

reported Ce stable isotopic variations in synthetic Ce/ferrihydrite and Ce/ δ -MnO₂ systems, and proposed that the Ce stable isotopic ratios can be used as a paleo-redox proxy. Subsequently, large Ce stable isotopic variations have also been observed in natural samples.^{8–13} The currently available data shows that the $\delta^{142/140}\text{Ce}$ values vary from -0.330‰ in Fe precipitates to 0.295‰ in marine ferromanganese oxides.⁹ According to the Eh–pH diagrams, Fe should be precipitated under reductive conditions, whereas Mn precipitates under oxidative conditions.^{9,14} The large difference in the $\delta^{142/140}\text{Ce}$ values of Fe (hydr-) oxides and Mn oxides indicates that the $\delta^{142/140}\text{Ce}$ value is a novel proxy to trace the redox evolution of the Earth's environment.^{9,15}

Like Ce, Nd is also a lithophile and refractory REE. It has seven natural isotopes, ^{142}Nd (27.152%), ^{143}Nd (12.174%), ^{144}Nd (23.798%), ^{145}Nd (8.293%), ^{146}Nd (17.189%), ^{148}Nd (5.756%) and ^{150}Nd (5.638%).¹ Among them, ^{142}Nd and ^{143}Nd both have radiogenic isotopic variations, which are the daughter products of radioactive ^{146}Sm ($T_{1/2} = 103 \text{ Ma}$ (ref. 16) or 68 Ma (ref. 17)) and ^{147}Sm ($T_{1/2} = 106 \text{ Ga}$ (ref. 18)), respectively. The other five isotopes are stable and only fractionated by mass dependent processes. Radiogenic Nd isotope geochemistry has been successfully applied in Earth and planetary sciences,^{19–25} marine

^aState Key Laboratory of Isotope Geochemistry, CAS Center for Excellence in Deep Earth Science, Guangzhou Institute of Geochemistry, Chinese Academy of Sciences, Guangzhou 510640, China. E-mail: jlma@gig.ac.cn

^bSouthern Marine Science and Engineering Guangdong Laboratory, Guangzhou 511458, China

^cNational-Regional Joint Engineering Research Center for Soil Pollution Control and Remediation in South China, Guangdong, Key Laboratory of Integrated Agro-environmental Pollution Control and Management, Institute of Eco-environmental and Soil Sciences, Guangdong Academy of Sciences, Guangzhou 510650, China

^dUniversity of Chinese Academy of Sciences, Beijing 100049, China

† Electronic supplementary information (ESI) available. See <https://doi.org/10.1039/d2ja00082b>

Table 1 Comparison of stable Ce and Nd isotope analytical methods^a

Separation method	Instruments	Ce				Nd				Column time	Ref.
		Residual		Residual		Residual		Residual			
		Yield	Nd	Blank	2SD	Yield	Ce	Blank	2SD		
One column: AG50W-X8 resin	TIMS + DS (¹⁴⁵ Nd + ¹⁵⁰ Nd)	+++	+++	+++	+++	—	0.03‰	—	0.03‰	—	Wakaki and Tanaka ³¹
Two columns: AG50W-X12 + Ln resin	Neptune Plus MC-ICP-MS	+++	+++	+++	+++	98.3%	4.4%	—	0.05‰	—	Ma <i>et al.</i> ³⁹
Three columns: AG50W-X8 + TRUSpec + Nu Plasma 500 MC-ICP-MS Ln resin	Nu Plasma 500 MC-ICP-MS	99%	<0.1%	1000 pg	0.08‰	95%	—	1000 pg	0.06‰	—	Ohno and Hirata ⁸
Three columns: AG50W-X8 + Ln(BrO ₃ ⁻); Neptune MC-ICP-MS H ₂ O ₂ + AG50W-X8	Neptune MC-ICP-MS	99%	~0.1%	—	0.04‰	+++	+++	+++	+++	—	Nakada <i>et al.</i> ^{4,9,10}
Four columns: AG50W-X8 + Ln + Ln + AG50W-X8 resin	Nu HR MC-ICP-MS Neptune Plus MC-ICP-MS	—	—	—	0.07‰	+++	+++	+++	+++	+++	Laycock <i>et al.</i> ¹³ Saji <i>et al.</i> ⁴⁰
One column: TODGA	Neptune Plus MC-ICP-MS	99.5%	0.05%	200 pg	0.04‰	+++	+++	+++	+++	7 h	Liu <i>et al.</i> ¹²
Two columns: AG50W-X8 + Ln resin	Triton Plus TIMS DS(¹⁴⁵ Nd + ¹⁵⁰ Nd)	+++	+++	+++	+++	96.8%	6%	3–55 pg	0.02‰	—	McCoy-West <i>et al.</i> ^{34,36}
One column: TODGA resin	Nu Plasma II MC-ICP-MS	+++	+++	+++	+++	99.2%	0.5%	30–70 pg	0.030	10 h	Wang <i>et al.</i> ⁵²
Three columns: AG50W-X8 + Ln(BrO ₃ ⁻); Triton Plus TIMS TS (¹³⁶ Ce + ¹³⁸ Ce + ¹⁴⁰ Ce)	Triton Plus TIMS TS (¹³⁶ Ce + ¹³⁸ Ce + ¹⁴⁰ Ce)	99%	—	500 pg	0.03–0.1‰	+++	+++	+++	+++	+++	Bonnand <i>et al.</i> ⁵⁰
Four columns: AG1-X8 + AG50W-X8 + HDEHP(BrO ₃ ⁻); H ₂ O ₂ + AG50 W-X8	Nu Plasma II MC-ICP-MS	—	—	—	0.13‰	+++	+++	+++	+++	+++	Pourkhorsandi <i>et al.</i> ¹¹
One column: TODGA	Neptune Plus MC-ICP-MS	+++	+++	+++	+++	99.5%	<0.04%	<50 pg	0.03‰	10 h	Bai <i>et al.</i> ⁵⁵
Two columns: AG50W-X12 + TODGA	Neptune Plus MC-ICP-MS	99.3%	<0.03%	<50 pg	0.04‰	99.5%	<0.04%	<50 pg	0.03‰	14 h	This work

^a DS = double spike; TS = three spike; +++ = cannot be studied. — = is not reported.

science,^{26–29} deposits,³⁰ and so on. By comparison, stable Nd isotope geochemistry ($\delta^{146/144}\text{Nd}$) is still in its infancy. Initially reported by Wakaki and Tanaka,³¹ large Nd stable isotopic fractionation has been observed above up to 1.404‰ in cation exchange column chromatography. Recently, this fractionation (about 0.25‰) has also been observed in natural samples, and has been applied with success in magmatic differentiation,^{32–35} early evolution of the Earth³⁶ and sediment provenances.³⁷ From this point of view, stable Nd isotopes can provide new insights in many scientific fields and is uncovering a new set of tools in geochemical studies.

Combined studies of stable isotopic systems of Ce and Nd have an important advantage because Ce and Nd behave similarly in geological processes and distinctively in redox reactions. Cerium (Ce) can be present as Ce(III), like Nd(III), as well as Ce(IV) under oxic conditions.³⁸ This difference can make the degree of stable Nd isotopic fractionations as a reference to better decipher the redox conditions of the stable Ce isotopic fractionations that occur in natural systems.⁸ Generally, Ce and Nd in natural rocks are purified by completely different methods, including four elution schemes (Table 1): (1) the classical two column AG50W + LN,^{36,39,40} tandem column TRU + LN I^{8,41,42} or TRU + LN II;^{43,44} (2) α -HIBA technique;^{3,31,45,46} (3) the NaBrO₃ method, also called liquid–liquid micro-extraction (LLME);^{2,47–51} (4) the single TODGA resin column.^{52–55} For the elution scheme (1), this method has not been applied to the study of Ce and Nd stable isotopes because 100% yield with perfect Ce–Nd separation is not achieved well (see Table S1 in Bai *et al.*⁵⁵). For example, Pin and Gannoun⁴³ presented a triple tandem column extraction for the isolation of highly purified Nd, but the chemical recoveries were between 80% and 90% in natural rocks. The incomplete Nd yield during chemical separation will result in mistaken information for stable Nd isotopic analyses when not using a double spike.^{31,55} For the elution scheme (2), in an original paper, Tanaka and Masuda³ presented a protocol for Ce separation using cation-exchange column chromatography with an α -HIBA reagent. This method was subsequently applied by several researchers to separate Nd.^{24,31,45,46,56} However, the α -HIBA chemistry suffers from several limitations when it is applied to stable Ce and Nd isotope purifications. For example, the pH value of α -HIBA needs to be well calibrated because the elution bands of La, Ce, Pr and Nd are very close. In fact, low yield and residual isobaric elements, such as Ce in Nd cuts, have been reported,^{45,46} which can severely impact the accuracy and precision of the measurements of stable Ce and Nd isotopes.^{12,55} In addition, a long and thin column (0.2 cm \times 20 cm)⁴⁵ was used in their method, which is time-consuming (\sim 4 days).^{31,46} For the elution scheme (3), Rehkämper *et al.*⁴⁷ reported a two-phase micro-extraction technique for the separation of Ce from the other LREEs, which can be called the NaBrO₃ method⁵⁷ or liquid–liquid micro-extraction (LLME).⁵¹ In their procedure, cerium (Ce) was oxidized from Ce(III) to Ce(IV) with NaBrO₃ in 10 M HNO₃ and then Ce(IV) was preferentially absorbed onto the organic phase. Further modification of the NaBrO₃ method was developed by other researchers.^{2,9–11,48–50} However, the inconveniences of this method have not been well solved, including (i) the non-reproducibility of the Nd yield (80–

100%), which is a noticeable phenomenon for stable Nd isotope analyses; (ii) the residual 10–20% Pr in the Nd cuts, which may cause the molecular interference of ¹⁴¹PrH on ¹⁴²Nd,⁴⁰ and data on stable Nd isotopes using the NaBrO₃ method has not been reported so far; (ii) the use of inorganic oxidizing agents (KBrO₃ or NaBrO₃) and concentrated HNO₃, which may cause higher blanks (\sim 500 pg)⁵⁰ and are not easy to operate. For elution scheme (4), some researchers recently reported the use of a TODGA resin column to purify Ce¹² or Nd,^{52–54} which has a very high efficiency for LREEs. For example, Bai *et al.*⁵⁵ established a single TODGA resin column to separate Nd from the other REEs. However, this method cannot be applied to purify Ce for the determination of Ce isotopic compositions because of the overlapping La–Ce–Pr bands (see Fig. 1 in Bai *et al.*⁵⁵). Residual La can cause large isobaric interference on Ce isotopes, and residual Pr may generate molecular interference from ¹⁴¹PrH on ¹⁴²Ce,^{12,40} and achieving very high Ce purity is of paramount importance. Taken together, all the techniques mentioned above suffer from two main problems: (1) two completely independent methods were employed to purify Ce and Nd from the other matrix elements, which is tedious and results in a high cost; (2) all these published elution schemes do not meet the requirement of a perfect separation of La–Ce–Pr–Nd, along with a nearly 100% recovery, which is essential to study the stable Ce and Nd isotopic ratios when not using a double spike during MC-ICP-MS measurements.

Here, we describe a novel two-stage chromatographic extraction technique that allows us to purify Ce and Nd from the same sample solution for the measurement of their isotopic ratios using MC-ICP-MS. The technique has several advantages: (1) a perfect La–Ce–Pr–Nd separation was achieved with the recoveries of Ce and Nd both being above 99.3%, which provides a practical method for the combined study of stable Ce and Nd isotopes; (2) Ce and Nd were purified by only one method, which minimizes the systematic errors and the consumptions and heterogeneities of the samples, which is of particular importance for meteorites and deep-sea materials; (3) only inorganic HNO₃ and HCl are used, without additional reagents, and concentrated HNO₃ (>8 M), which are easy to handle; (4) a cation exchange AG50W-X12 resin, instead of TODGA resin, was selected to remove the major matrix elements (Ca, Mg, Fe, K, *etc.*) because the latter is about six times more expensive than the former. Furthermore, different geological rocks, including basalt, andesite, granodiorite, granite, rhyolite, manganese nodule and dolomite, were analysed to examine the efficacy of this technique.

2. Experimental sections

2.1 Reagents and materials

BV-III grade HCl, HF, and HNO₃ were single-distilled in a DST-1000 system (Saville, USA). Ultra-pure water with a resistivity of 18.2 M Ω cm was produced by a Milli-Q system (USA). The single element REE solutions (1000 $\mu\text{g g}^{-1}$) were obtained from the Beijing General Research Institute for Nonferrous Metals. A synthetic solution was made from a mixture of 15 single-element solutions (La : Ce : Pr : Nd : Sm : Eu : Gd : Tb : Dy :

22 mL of 2.8 M HCl to elute Ce, 21 mL of 2.5 M HCl to elute Pr, 10 mL of 1.5 M HCl to elute Nd, and finally 15 mL of 0.1 M HCl to elute the other REEs (Sm–Lu). The yields of Ce and Nd were both nearly 100% after actual measurements, which were checked by testing the pre-cut and post-cut aliquots of Ce and Nd using inductively coupled plasma mass spectrometry (ICP-MS) at the State Key Laboratory of Isotope Geochemistry (SKLaBIG), Guangzhou Institute of Geochemistry, Chinese Academy of Sciences (GIG-CAS). The ICP-MS operating conditions and the yield data are listed in Tables S1 and S2,[†] respectively. Both the purified Ce and Nd cuts were dried and finally redissolved in 2% HNO₃ for their stable isotope measurements. The Ce and Nd blank contributions from the digestion and two-column procedures were 48 pg and 33 pg, respectively.

2.3 Mass spectrometry

Both stable Ce and Nd isotopic ratios were measured on a Thermo Fisher Scientific Neptune Plus MC-ICP-MS at the SKLaBIG, GIG-CAS. The typical operating conditions of this instrument for the Ce and Nd isotopic analysis are listed in Table 3. All measurements were carried out in a low mass resolution (~400) and static mode. Sample solutions in 2%

HNO₃ were introduced into the plasma using a self-aspiration capillary PFA nebulizer (50 μL min⁻¹) and a dual cyclonic-Scott spray chamber. Each analysis consisted of 60 cycles with an integration time of 4.194 s.

The combined standard-sampled bracketing and internal normalization (C-SSBIN) model was employed to correct the mass discrimination effect occurring in MC-ICP-MS instruments. The principles for selecting an internal standard are that it is the closest to the target element in mass and does not cause isobaric interference.⁵⁸ For Ce isotopic analysis, Sm is the most suitable internal standard because La and Nd both have isobaric interference on Ce. As such, Eu is the best calibrator for the Nd isotopic measurements. During Ce isotopic measurements, the cups L4, L3, L2, L1, C, H1, H2, and H3 were used to collect ¹³⁹La, ¹⁴⁰Ce, ¹⁴¹Pr, ¹⁴²Ce, ¹⁴³Nd, ¹⁴⁵Nd, ¹⁴⁷Sm and ¹⁴⁹Sm, simultaneously. ¹⁴⁵Nd was used to examine the isobaric interference of ¹⁴²Nd on ¹⁴²Ce with ¹⁴²Nd/¹⁴⁵Nd = 3.27409. ¹⁴⁹Sm/¹⁴⁷Sm = 0.92195 (ref. 59) was used as the normalization value. Because Ce can be easily oxidized at the ICP interface under wet plasma conditions,⁹ the ratio of CeO/Ce should be suppressed to lower than 2% by turning the operating conditions of the instrument. A mixture of standard solutions including 100 ng g⁻¹ Ce and 100 ng g⁻¹ Sm was adopted as the

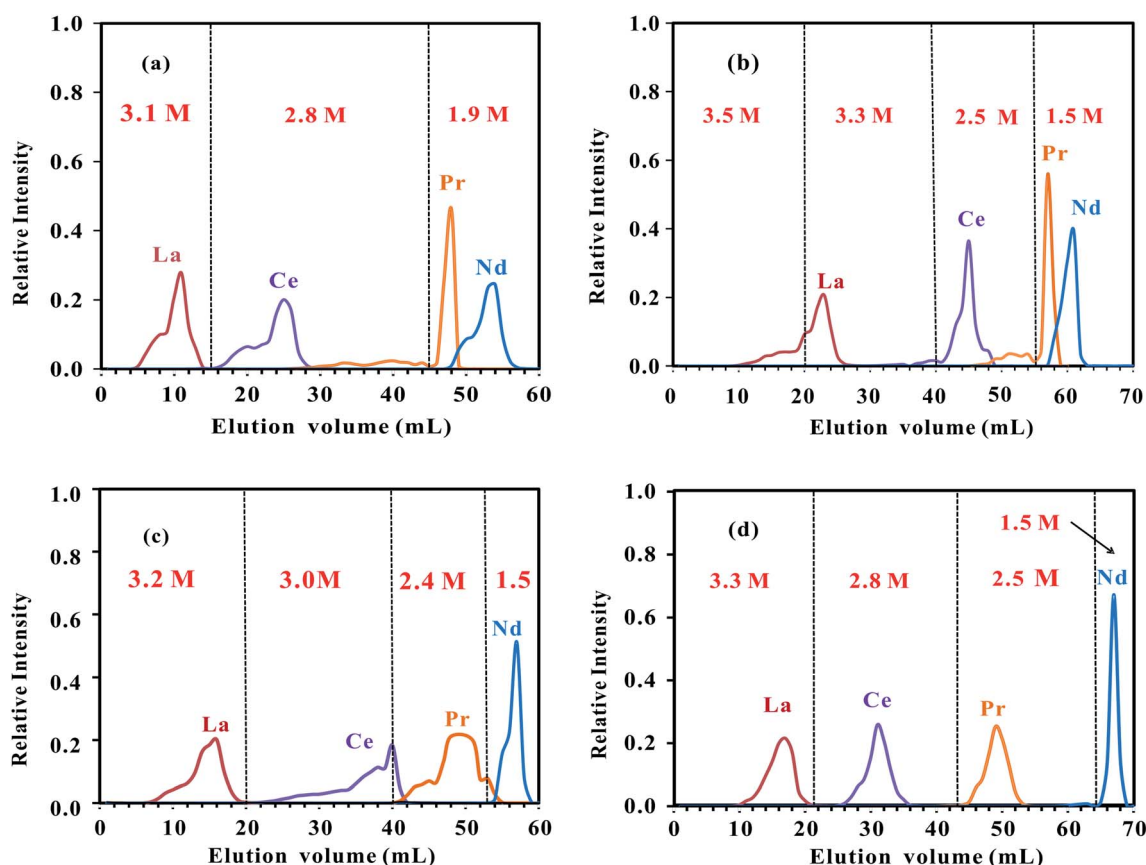


Fig. 1 The four typical elution curves of La, Ce, Pr and Nd using different volumes and molarities of HCl on a column filled with 2 mL of Eichrom TODGA resin (50–100 μm), (a) the first test; (b) the second test; (c) the third test and (d) the fourth test. The figure shows that the peaks of La, Ce, Pr and Nd were very sensitive to the volumes and molarities of HCl, and the fourth scheme (d) should be adopted. The synthetic multi-elemental solution (La : Ce : Pr : Nd : Sm : Eu : Gd : Tb : Dy : Ho : Er : Tm : Yb : Lu : Y = 2 : 3 : 1 : 2 : 1 : 1 : 1 : 1 : 1 : 1 : 1 : 1 : 1 : 1 : 1) was adopted to obtain the curves.

reference standard, which provided ^{140}Ce and ^{147}Sm signals of 8.5 V and 1.2 V, respectively. For Nd isotopic measurements, the cups L4, L3, L2, L1, C, H1, H2, and H3 were used to collect ^{140}Ce , ^{142}Nd , ^{143}Nd , ^{144}Nd , ^{145}Nd , ^{146}Nd , ^{151}Eu and ^{153}Eu , simultaneously. ^{140}Ce was used to examine the isobaric interference of ^{142}Ce on ^{142}Nd with $^{142}\text{Ce}/^{140}\text{Ce} = 0.12589$.² $^{153}\text{Eu}/^{151}\text{Eu} = 1.09160$ (ref. 60) was used as the normalization value. The mixture of standard solutions including 200 ng g⁻¹ Nd and 48 ng g⁻¹ Eu provided ^{144}Nd and ^{153}Eu signals of 3.5 V and 1.8 V, respectively. To avoid the influence of mismatching concentrations, all the samples introduced into the instruments were carefully adjusted to within 10% difference of the mixture of standard solutions. Cerium (Ce) and Nd isotopic compositions are expressed in the usual delta notation $\delta^{142/140}\text{Ce}$ and $\delta^{146/144}\text{Nd}$, respectively, as given below:

$$\delta^{142/140}\text{Ce} = \left[\frac{(^{142}\text{Ce}/^{140}\text{Ce})_{\text{sample}}}{(^{142}\text{Ce}/^{140}\text{Ce})_{\text{NIST3110}}} - 1 \right] \times 1000 \quad (1)$$

$$\delta^{146/144}\text{Nd} = \left[\frac{(^{146}\text{Nd}/^{144}\text{Nd})_{\text{sample}}}{(^{146}\text{Nd}/^{144}\text{Nd})_{\text{JNdi-1}}} - 1 \right] \times 1000 \quad (2)$$

where NIST 3110 is used as the reference standard for Ce and JNdi-1 for Nd, respectively.

3. Results and discussions

3.1 Effect of acid on La, Ce, Pr and Nd elution

In order to obtain an optimal configuration of the acid and avoid potential contamination, different volumes and molarities of HCl were thoroughly investigated. Our first test used 15 mL of 3.1 M HCl to purify La, 30 mL of 2.8 M HCl to purify Ce and Pr, and 15 mL of 1.9 M HCl to purify Nd. The results showed that perfect La-Ce separation was achieved (Fig. 1a). However, the separation of Pr and Nd could not be achieved in this test. Moreover, Fig. 1a shows that Pr³⁺ and Nd³⁺ have a similar affinity for the Eichrom TODGA resin in 1.9 M HCl, and Pr³⁺ has a strong retention on this resin in 2.8 M HCl media. Molarities of acid lying between 2.8 M to 1.9 M thus should be used to purify Pr from Ce and Nd. Our second test, using four acid molarities of 3.5 M HCl, 3.3 M HCl, 2.5 M HCl and 1.5 M HCl, predictably achieved excellent La-Ce-Pr-Nd separations. Unexpectedly, as shown in Fig. 1b, large overlaps of the cuts of Ce-Pr-Nd occurs in this elution profile. However, several important points were also noted in this procedure, especially the behavior of La³⁺, Ce³⁺ and Sm³⁺ in HCl media.

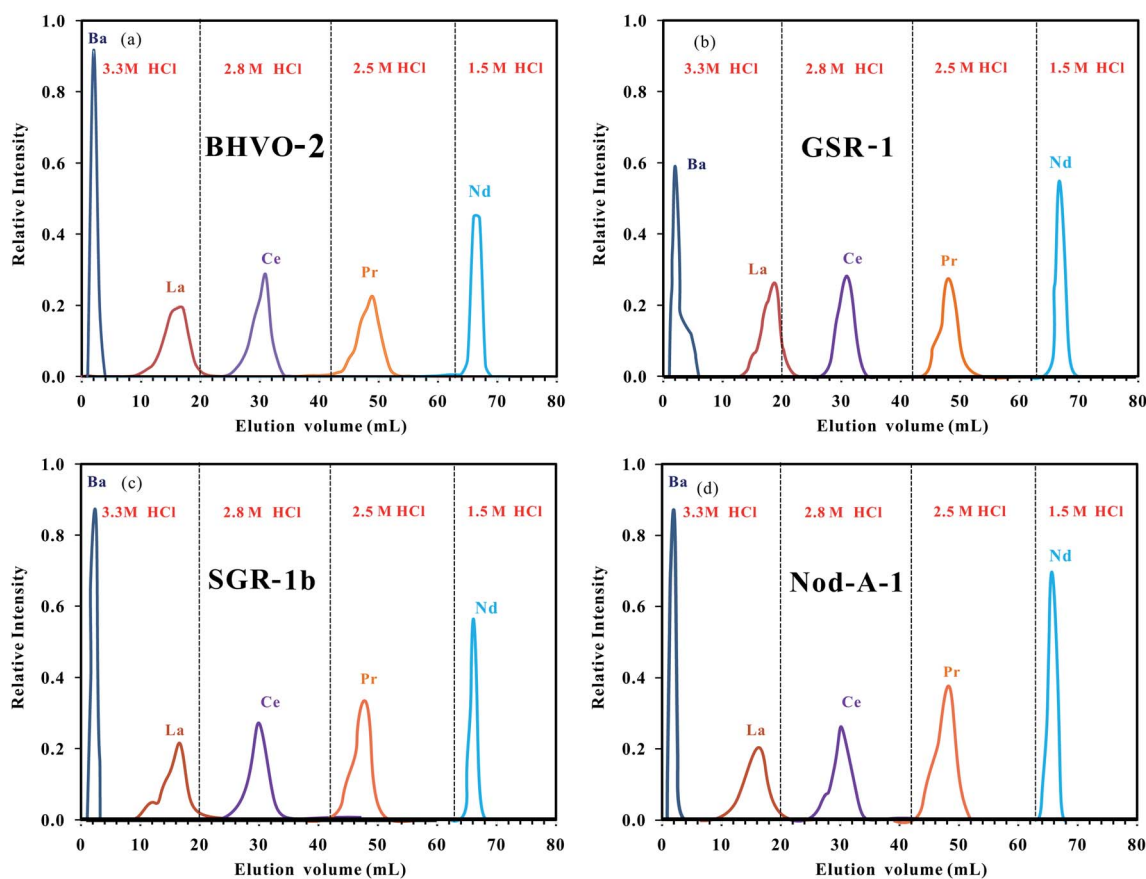


Fig. 2 Elution curves of Ba, La, Ce, Pr and Nd purification procedures using different rock types, (a) BHVO-2; (b) GSR-1; (c) SGR-1b and (d) Nod-A-1, with the same Nd content (1 μg) on the Eichrom TODGA column. Despite the different sets of matrix elements, the element peaks of BHVO-2, SGR-1b, GSR-1, and Nod-A-1 were eluted in the same sections.

La³⁺ has a relatively strong affinity for Eichrom TODGA resin in >3.5 M HCl (Fig. 1b) but a weak retention in <3.1 M HCl (Fig. 1a). Ce³⁺ has a strong retention on Eichrom TODGA resin in >3.3 M HCl media (Fig. 1b) but a weak affinity in <2.8 M HCl. Sm³⁺ cannot be eluted from the TODGA column together with Nd due to the fact that it has a much stronger affinity for this resin with 1.5 M HCl elution (not shown in Fig. 1). A perfect separation of Nd from Sm thus can be achieved with 1.5 M HCl media. For our third test, 20 mL of 3.3 M HCl, 20 mL of 3.0 M HCl, 15 mL of 2.4 M HCl and 15 mL of 1.5 M HCl were applied to further isolate La–Ce–Pr–Nd from the other REEs. It was found that Ce retains a relatively strong affinity for Eichrom TODGA resin in 3.0 M HCl (Fig. 1c), as well as the Pr cut overlapping with the Nd cut. For our fourth test, 20 mL of 3.3 M HCl was used to elute La, 22 mL of 2.8 M HCl to elute Ce, 21 mL of 2.5 M HCl to elute Pr, 10 mL of 1.5 M HCl to elute Nd (Fig. 1d), and 15 mL of 0.1 M HCl to elute the other REEs (not shown in Fig. 1). As shown in Fig. 1d, a perfect separation of the individual REEs (La, Ce, Pr and Nd) from each other could be achieved. It is noteworthy that this method was sensitive to the molarity of HCl, and thus the HCl content should be carefully calibrated using standard NaOH solution before using it.

3.2 Effect of rock types with different Ce/Nd ratios

Previous studies on other stable metal isotopes,^{55,61–63} such as Mg, have shown that the elution profile could shift due to the various matrix/target element ratios. To further test the reliability of the elution curve, four types of rocks, including basalt standard BHVO-2 with a Ce/Nd ratio of 1.5, granite GSR-1 with a Ce/Nd ratio of 2.3, shale powder SGR-1b with a Ce/Nd ratio of 2.5 and manganese nodule Nod-A-1 with a Ce/Nd ratio of 7.8, were selected. Each of the samples contained the same amount of Nd (1 μg) with different Ce/Nd ratios, ranging from 1.5 to 7.8, which covers the majority of natural samples (Ce/Nd ratios ranging from 1.5 to 5). After sample loading, the eluate was continuously collected, 1 mL by 1 mL, and then was measured for trace elements, including REEs, by ICP-MS at SKLaBIG, GIG-CAS. As shown in Fig. 2, all samples processed through our column procedure have similar elution peaks, proving that this procedure is robust to different rock types. At the initial stage of the development of this procedure, we did not take into account Ba in our synthetic solutions because it has very weak retention on TODGA resin in HCl media.⁶⁴ Indeed, Ba also had little discernible effect

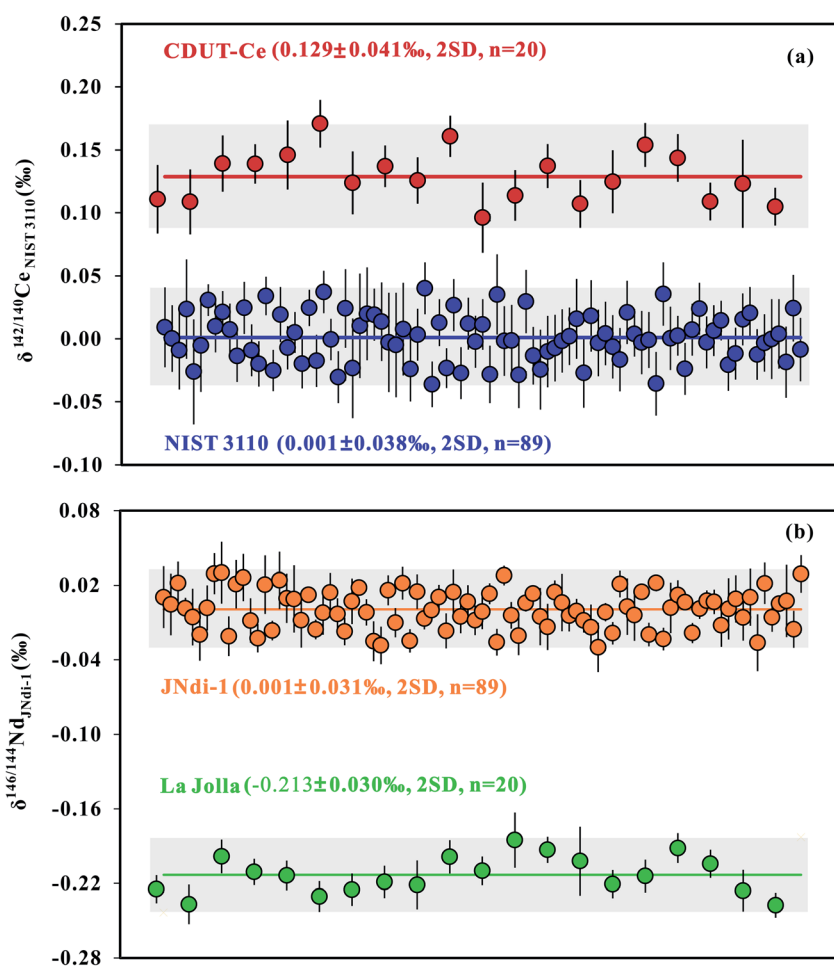


Fig. 3 Long-term reproducibility of (a) the standard solutions NIST 3110 and CDUT-Ce for Ce isotopic analysis and (b) the standard solutions JNdi-1 and La Jolla for Nd isotopic analysis, measured on a Neptune Plus MC-ICP-MS instrument at GIG-CAS.

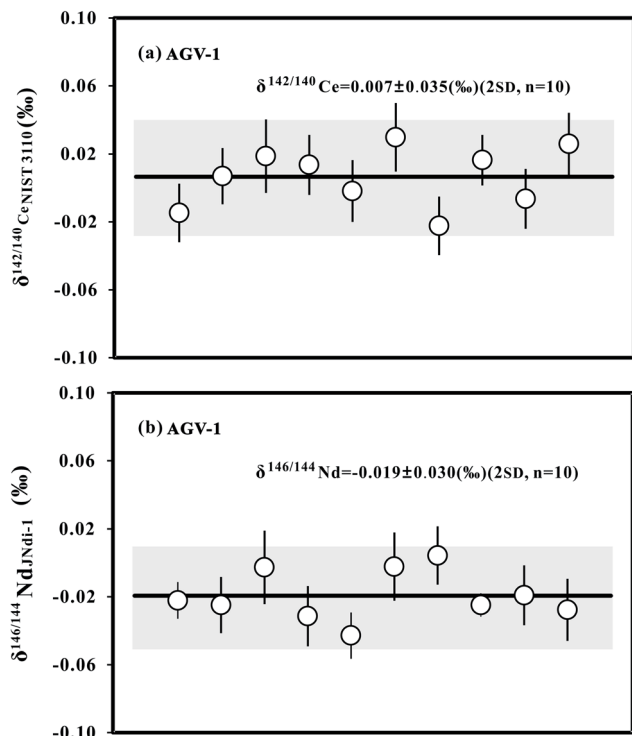


Fig. 4 Long-term reproducibility of the USGS rock AGV-1 replicated digestion and processed through the column chemistry and analyzed separately for Ce (a) and Nd (b) isotope measurements. The complete dataset can be obtained from Table 4. The reproducibilities of $\delta^{142/140}\text{Ce}$ and $\delta^{146/144}\text{Nd}$ analyzed here are better than $\pm 0.04\%$ and $\pm 0.03\%$, respectively.

on the elution peaks of La, Ce, Pr, and Nd (Fig. 2). Moreover, no detectable influences on matrix elements, including Ba, could be found in each of the individual La, Ce, Pr and Nd fractions. These results further confirm that a perfect separation of multi-REEs (La, Ce, Pr and Nd) from the rest of the REEs can be achieved.

3.3 Precision and accuracy

The precision and accuracy of our method were assessed by conducting replicate measurements of the pure standard solutions and geological rocks. Repeated measurements of the pure Ce standard solutions NIST 3110 ($\delta^{142/140}\text{Ce} = 0.001 \pm 0.038\%$, 2SD, $n = 89$) and CDUT-Ce ($\delta^{142/140}\text{Ce} = 0.129 \pm 0.041\%$, 2SD, $n = 20$) at the SKLaBIG, GIG-CAS over an eight month period gave a stability better than $\pm 0.04\%$ (Fig. 3a). The stable Ce isotopic analysis measurements of CDUT-Ce here are within the uncertainty of that previously reported ($\delta^{142/140}\text{Ce} = 0.128 \pm 0.028\%$, 2SD, $n = 30$). Repeated measurements of the pure Nd standard solutions JNdi-1 ($\delta^{146/144}\text{Nd} = 0.001 \pm 0.031\%$, 2SD, $n = 89$) and La Jolla ($\delta^{146/144}\text{Nd} = -0.213 \pm 0.030\%$, 2SD, $n = 20$) gave a stability better than $\pm 0.03\%$ (Fig. 3b). The stable Nd isotopic analysis results of La Jolla measured here are within the uncertainties of those previously reported by Wakaki and Tanaka³¹ ($\delta^{146/144}\text{Nd} = -0.197 \pm 0.023\%$, 2SD, $n = 2$), Saji *et al.*⁴⁰ ($\delta^{146/144}\text{Nd} = -0.243 \pm 0.040\%$, 2SD, $n = 3$), McCoy-West *et al.*³⁴ ($\delta^{146/144}\text{Nd} = -0.214 \pm 0.010\%$, 2SD, $n = 7$), and Bai *et al.*⁵⁵ ($\delta^{146/144}\text{Nd} = -0.227 \pm 0.030\%$, 2SD, $n = 20$). The long-term reproducibility of the technique was tested further through ten repeated digestions of AGV-1, and processed through the

Table 4 Stable Ce and Nd isotopic compositions of the standard solutions and geological samples measured in the current study

Sample	Description	Ce ^a ($\mu\text{g g}^{-1}$)	¹⁴⁵ Nd/ ¹⁴² Ce	$\delta^{142/140}\text{Ce}$	2SD ^b	N ^c	Nd ^a ($\mu\text{g g}^{-1}$)	¹⁴⁰ Ce/ ¹⁴⁴ Nd	$\delta^{146/144}\text{Nd}$	2SD ^b	N ^c
NIST 3110	Ce standard	—	0.00002	0.001	0.038	89	—	—	—	—	—
CDUT-Ce	CeO ₂	—	0.00005	0.129	0.041	20	—	—	—	—	—
JNdi-1	Nd standard	—	—	—	—	—	—	0.00005	0.001	0.031	89
La Jolla	Nd standard	—	—	—	—	—	—	0.00005	-0.213	0.030	20
BHVO-2	Basalt	37.5	0.00008	0.000	0.046	3	24.3	0.00170	-0.029	0.018	3
BCR-2	Basalt	53.1	0.00006	0.010	0.037	3	28.2	0.00176	-0.048	0.028	3
BCR-2-(2) ^d	—	—	0.00009	0.006	—	1	—	0.00247	-0.036	—	1
AGV-2	Andesite	69.4	0.00009	-0.018	0.042	3	30.5	0.00237	-0.020	0.020	3
AGV-1	Andesite	68.5	0.00010	-0.015	0.036	3	32.3	0.00154	-0.022	0.029	3
AGV-1-(2)	—	—	0.00005	0.007	—	1	—	0.00211	-0.025	—	1
AGV-1-(3)	—	—	0.00008	0.019	—	1	—	0.00311	-0.003	—	1
AGV-1-(4)	—	—	0.00010	0.014	—	1	—	0.00197	-0.031	—	1
AGV-1-(5)	—	—	0.00013	-0.002	—	1	—	0.00258	-0.043	—	1
AGV-1-(6)	—	—	0.00005	0.030	—	1	—	0.00314	-0.002	—	1
AGV-1-(7)	—	—	0.00004	-0.022	—	1	—	0.00168	0.004	—	1
AGV-1-(8)	—	—	0.00004	0.016	—	1	—	0.00142	-0.025	—	1
AGV-1-(9)	—	—	0.00005	-0.006	—	1	—	0.00178	-0.019	—	1
AGV-1-(10)	—	—	0.00006	0.026	—	1	—	0.00198	-0.028	—	1
Average ($n = 10$)	—	—	—	0.007	0.035	—	—	—	-0.019	0.030	—
GSP-2	Granodiorite	410	0.00013	0.022	0.035	3	200	0.00184	-0.038	0.024	3
GSR-1	Granite	108	0.00010	0.028	0.034	3	47	0.00152	0.005	0.028	3
GSR-11	Rhyolite	163	0.00006	0.033	0.044	3	64.5	0.00284	0.014	0.031	3
Nod-P-1	Mn nodule	292	0.00007	0.112	0.046	3	120	0.00267	0.024	0.029	3
Nod-A-1	Mn nodule	731	0.00015	0.131	0.042	3	94	0.00192	0.013	0.032	3
JDo-1	Dolomite	2.5	0.00021	0.143	0.041	3	5.3	0.00085	0.128	0.031	3

^a The contents of Ce and Nd are taken from <https://georem.mpch-mainz.gwdg.de/>. ^b 2SD = 2 standard deviations. ^c N denotes the number of repeated analyses of the same solutions. ^d () is a separate digestion and independent processing through the complete separation protocol.

column chemistry plus analysis (Fig. 4). The geological sample AGV-1 had reproducibilities better than $\pm 0.040\text{‰}$ for $\delta^{142/140}\text{Ce}$ (Fig. 4a) and $\pm 0.030\text{‰}$ for $\delta^{146/144}\text{Nd}$ (Fig. 4b).

In order to assess the accuracy of the method established here, six well-studied samples, BHVO-2, BCR-2, AGV-2, AGV-1, GSP-2 and JDo-1, were measured in this study (Table 4). The values (means $\pm 2\text{SD}$) of $\delta^{142/140}\text{Ce}$ were $0.000 \pm 0.046\text{‰}$ for BHVO-2, $0.010 \pm 0.037\text{‰}$ for BCR-2, $-0.018 \pm 0.042\text{‰}$ for AGV-2, $0.007 \pm 0.035\text{‰}$ for AGV-1, $0.022 \pm 0.035\text{‰}$ for GSP-2 and $0.143 \pm 0.041\text{‰}$ for JDo-1. These results are in agreement within uncertainty with those reported by other researchers (Fig. 5a).^{8,10,12} The $\delta^{146/144}\text{Nd}$ values (means $\pm 2\text{SD}$) for BHVO-2, BCR-2, AGV-2, AGV-1, GSP-2 and JDo-1 were $-0.029 \pm 0.018\text{‰}$, $-0.048 \pm 0.028\text{‰}$, $-0.020 \pm 0.020\text{‰}$, $-0.019 \pm 0.030\text{‰}$, $-0.038 \pm 0.024\text{‰}$, $0.128 \pm 0.031\text{‰}$, which agreed with the available literature data (Fig. 5b).^{34,36,55} Taken together, these data demonstrate the reliability of our method.

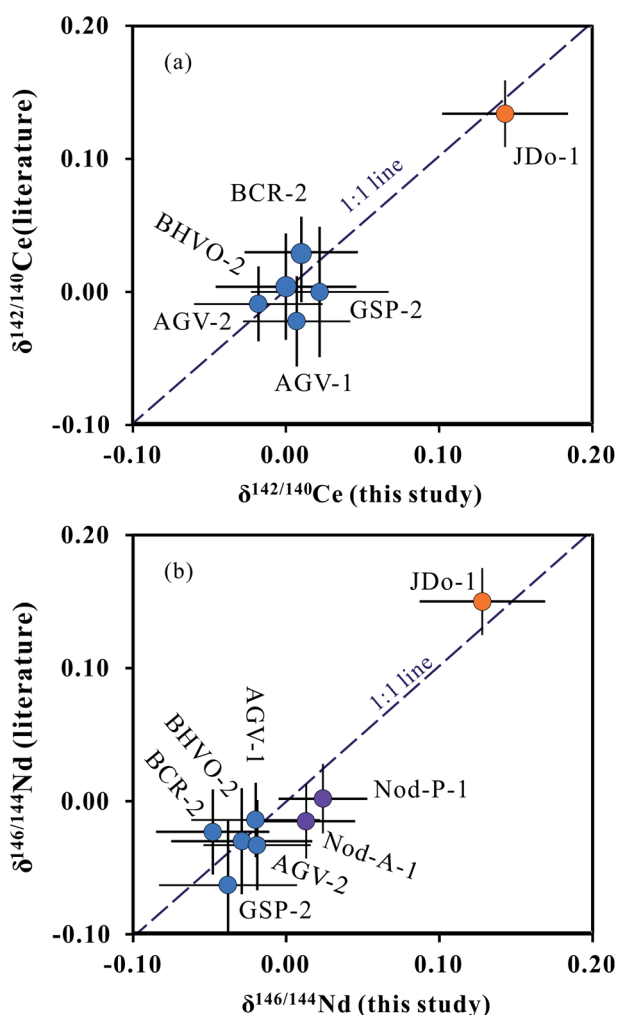


Fig. 5 Comparison of Ce (a) and Nd (b) isotopic compositions of geological reference materials reported in this study and those reported in the literature. The data from this study are listed in Table 4. Cerium (Ce) isotopic data are taken from Nakada *et al.*¹⁰ and Liu *et al.*,¹² and Nd isotopic data are taken from Ohno and Hirata,⁸ McCoy-West *et al.*³⁴ and Bai *et al.*⁵⁵

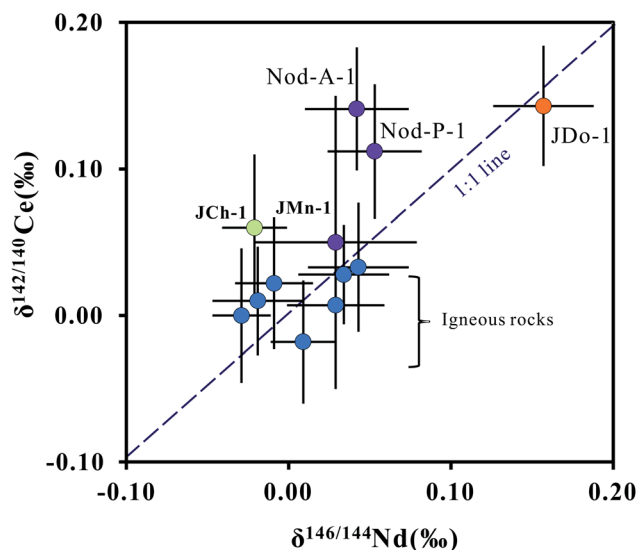


Fig. 6 Stable Ce and Nd isotopic compositions of geological rocks. Blue circles are igneous rocks, including basalt, andesite, granodiorite, granite and rhyolite, measured in this study. Purple circles are the manganese nodules JMn-1, Nod-P-1 and Nod-A-1. The JMn-1 values were reported in a previous work,⁸ while Nod-P-1 and Nod-A-1 were measured by this present study. The green circle is chert JCh-1, taken from Ohno and Hirata.⁸ The brown circle is the marine dolomite JDo-1 measured in this study. Since Pourkhorasandi *et al.*¹¹ used Ames Ce as a reference rather than NIST 3110 or JMC 304, their data were not discussed due to the fact that the $\delta^{142/140}\text{Ce}$ value between Ames Ce and NIST 3110 or JMC 304 is unknown. Each of stable Ce and Nd isotopic data were normalized by BHVO-2 in this study. All error bars represent two standard deviations of the mean.

3.4 $\delta^{142/140}\text{Ce}$ and $\delta^{146/144}\text{Nd}$ values for geological reference materials

Using the column separation method established here, we reported the stable Ce and Nd isotopic compositions of ten geological rocks, including basalt, andesite, granodiorite, granite, rhyolite, Mn nodule and dolomite. The final results are presented in Table 4 and shown in Fig. 6. The $\delta^{142/140}\text{Ce}$ and $\delta^{146/144}\text{Nd}$ results of igneous rocks range from -0.018‰ to $+0.033\text{‰}$ and -0.048‰ to $+0.014\text{‰}$, respectively, suggesting that both stable Ce and Nd do not fractionate markedly in high-temperature magmatic processes. They are in agreement with the earlier reported $\delta^{142/140}\text{Ce}$ and $\delta^{146/144}\text{Nd}$ values of igneous rocks.^{10,12,32,34,36,55} For the manganese nodules Nod-P-1 and Nod-A-1, their Nd isotopes also do not fractionate so much with the standard solution JNdi-1, which is consistent with the results from Bai *et al.*⁵⁵ In contrast, the two manganese nodules clearly showed heavier Ce enrichment, with $\delta^{142/140}\text{Ce}$ values of $0.112 \pm 0.046\text{‰}$ and $0.131 \pm 0.042\text{‰}$, respectively, which are the first reported. The difference in the magnitude of Ce and Nd isotopic fractionation could be attributed to the Ce(III) to Ce(IV) exchange reaction. According to the thermodynamic data, Ce(III) could be oxidized to Ce(IV) by Mn oxides.^{4,14} The Ce–O bond length of Ce(IV) is shorter than that of Ce(III)⁴ and, thus, heavier Ce isotopes are enriched. The $\delta^{142/140}\text{Ce}$ and $\delta^{146/144}\text{Nd}$ values of the manganese nodules JMn-1 ($0.05 \pm 0.10\text{‰}$ and $0.00 \pm 0.05\text{‰}$,

respectively) taken from Ohno and Hirata⁸ were not discussed due to their large uncertainties. Nakada *et al.*⁹ and Nakada *et al.*¹⁰ also measured JMn-1 and reported relatively heavier $\delta^{142/140}\text{Ce}$ values of $0.104 \pm 0.034\%$ and $0.110 \pm 0.025\%$, respectively. For dolomite JDo-1, earlier studies showed heavier Ce enrichment, with $\delta^{142/140}\text{Ce}$ values of $0.170 \pm 0.050\%$ ⁸ and $0.134 \pm 0.025\%$,¹⁰ respectively. The $\delta^{146/144}\text{Nd}$ value of JDo-1 is $0.150 \pm 0.040\%$, reported by Ohno and Hirata.⁸ The $\delta^{142/140}\text{Ce}$ and $\delta^{146/144}\text{Nd}$ values measured in the current study were $0.143 \pm 0.041\%$ and $0.128 \pm 0.031\%$, respectively, which are identical to earlier measurements within the analytical uncertainty. The similarity in the degree of Ce and Nd isotopic fractionation may be induced by the low-temperature carbonate processes rather than redox changes. The Nd isotopic fractionation factor between the ion-exchange resin and the solute (HIBA) at 24–28 °C was determined to be 0.999964.³¹ This indicates that the low-temperature equilibrium chemical reaction may generate Nd stable isotopic fractionation on the order of the 0.1‰ level. Similar features were also observed in Sm stable isotopic studies.⁶⁵ The dolomite JDo-1 from the Mesozoic seamount-type suggested the water–rock interaction also leads to the detectable Ce and Nd isotopic fractionation. The stable isotopic fractionations are usually controlled by multiple processes such as the redox reaction, ad/desorption, or precipitation and so on, which is difficult to unambiguously fingerprint the contribution of each process based on a single isotopic system.⁶⁶ Combined studies of stable isotopic systematics of Ce and Nd have an important advantage in geochemistry and can provide unique information about global redox states of paleo-marine environments.

4. Conclusions

A new two-stage column method was developed to purify Ce and Nd from the matrix elements for their stable isotopic analysis by MC-ICP-MS. This procedure results in four single element fractions (La, Ce, Pr, Nd), each with high recovery (>99.3%) and low whole procedure blanks (<50 pg). Several important parameters for the effectiveness of this method, such as the acid molarity and various rock types, were systematically examined. Combined standard-sample bracketing and the internal normalization isotopic fractionation correction model gave long-term external reproducibilities of better than $\pm 0.04\%$ (2SD) for $\delta^{142/140}\text{Ce}$ and $\pm 0.03\%$ (2SD) for $\delta^{146/144}\text{Nd}$. Using the technique established here, stable Ce and Nd isotopic ratios of ten commercially accessible geological rocks were measured. Among them, six well-studied samples yielded $\delta^{142/140}\text{Ce}$ and $\delta^{146/144}\text{Nd}$ values that were consistent with previously reported results, particularly with the double spike method. The data measured in the current study provide a case for combined studies of stable Ce and Nd isotopes, which will be a promising way to understand complicated geological processes. In addition, this technique, which uses the same aliquots for stable Ce and Nd isotopic analysis, is of paramount importance for samples that are limited in quantity, such as abyssal sediments, and that are heterogeneous in composition, such as meteoritic materials. Stable isotope studies of Ce and Nd remain in their

infancy and further developments will be expected with this technique.

Author contributions

J.-H. Bai and J.-L. Ma conceived the study. J.-H. Bai performed the experiments. G.-J. Wei and S.-X. Zhong contributed to the column chemistry. G.-J. Wei and L. Zhang contributed to the isotopic analysis. J.-H. Bai, J.-L. Ma and G.-J. Wei analyzed the data. J.-H. Bai wrote the manuscript with significant input from all co-authors.

Conflicts of interest

The authors declare no competing financial interest.

Acknowledgements

This work was funded by the Fundamental and Applied Fundamental Research Major Program of Guangdong Province (Grant No. 2019B030302013), National Natural Science Foundation of China (41991325, 42021002), Natural Science Foundation of Guangdong Province (Grant No. 2021A1515110574) and the Key Special Project for Introduced Talents Team of Southern Marine Science and Engineering Guangdong Laboratory (Guangzhou) (GML2019ZD0308). The authors thank the three anonymous reviewers for their constructive and helpful comments. We also appreciate the experimental help from Lei Zhang and Xianglin Tu. This is contribution No. IS-3203 from GIG-CAS.

References

- 1 M. Berglund and M. E. Wieser, *Pure Appl. Chem.*, 2011, **83**, 397–410.
- 2 M. Willig and A. Stracke, *Chem. Geol.*, 2018, **476**, 119–129.
- 3 T. Tanaka and A. Masuda, *Nature*, 1982, **300**, 515–518.
- 4 R. Nakada, Y. Takahashi and M. Tanimizu, *Geochim. Cosmochim. Acta*, 2013, **103**, 49–62.
- 5 A. P. Dickin, N. W. Jones, M. F. Thirlwall and R. N. Thompson, *Contrib. Mineral. Petrol.*, 1987, **96**, 455–464.
- 6 H. Shimizu, T. Tanaka and A. Masuda, *Nature*, 1984, **307**, 251–252.
- 7 M. Willig, A. Stracke, C. Beier and V. J. M. Salters, *Geochim. Cosmochim. Acta*, 2020, **272**, 36–53.
- 8 T. Ohno and T. Hirata, *Anal. Sci.*, 2013, **29**, 47–53.
- 9 R. Nakada, Y. Takahashi and M. Tanimizu, *Geochim. Cosmochim. Acta*, 2016, **181**, 89–100.
- 10 R. Nakada, N. Asakura and K. Nagaishi, *Geochem. J.*, 2019, **53**, 293–304.
- 11 H. Pourkhorsandi, V. Debaille, J. de Jong and R. M. G. Armytage, *Talanta*, 2021, **224**, 121877.
- 12 F. Liu, Z. Zhang, X. Li, Y. An, Y. Liu, K. Chen, Z. Bao and C. Li, *Anal. Chem.*, 2021, **93**, 12524–12531.
- 13 A. Laycock, B. Coles, K. Kreissig and M. Rehkämper, *J. Anal. At. Spectrom.*, 2016, **31**, 297–302.

- 14 D. G. Brookins, *Eh-pH diagrams for geochemistry*, Springer-Verlag, 1988.
- 15 R. Nakada, M. Tanimizu and Y. Takahashi, *Geochim. Cosmochim. Acta*, 2013, **121**, 105–119.
- 16 F. Meissner, W. D. Schmidt, L. Ziegeler and Z. Phys., *Z. Phys. A: At. Nucl.*, 1987, **327**, 171–174.
- 17 N. Kinoshita, M. Paul, Y. Kashiv, P. Collon, C. M. Deibel, B. DiGiovine, J. P. Greene, D. J. Henderson, C. L. Jiang, S. T. Marley, T. Nakanishi, R. C. Pardo, K. E. Rehm, D. Robertson, R. Scott, C. Schmitt, X. D. Tang, R. Vondrasek and A. Yokoyama, *Science*, 2012, **335**, 1614–1617.
- 18 G. W. Lugmair and K. Marti, *Earth Planet. Sci. Lett.*, 1978, **39**, 349–357.
- 19 R. E. Carlson, M. Boyet and M. Horan, *Science*, 2007, **316**, 1175–1178.
- 20 A. Gannoun, M. Boyet, H. Rizo and A. El Goresy, *Proc. Natl. Acad. Sci. U. S. A.*, 2011, **108**, 7693–7697.
- 21 D. J. DePaolo, Neodymium isotope geochemistry, *Minerals and Rocks*, Springer-Verlag, 1988.
- 22 F. Moynier, Q. Z. Yin, K. Irisawa, M. Boyet, B. Jacobsen and M. T. Rosing, *Proc. Natl. Acad. Sci. U. S. A.*, 2010, **107**, 10810–10814.
- 23 G. Caro, *Annu. Rev. Earth Planet. Sci.*, 2011, **39**, 31–58.
- 24 C. Burkhardt, L. E. Borg, G. A. Brennecke, Q. R. Shollenberger, N. Dauphas and T. Kleine, *Nature*, 2016, **537**, 394–398.
- 25 J. Bai, M. Ling, X. Yang, F. Liu, H. Gu, Z. Luo, X. Jiang and Z. Zhang, *J. Earth Sci.*, 2022, **33**, 581–590.
- 26 F. Albarede and S. L. Goldstein, *Geology*, 1992, **20**, 761–763.
- 27 T. van de Fliert, S. L. Goldstein, S. R. Hemming, M. Roy, M. Frank and A. N. Halliday, *Earth Planet. Sci. Lett.*, 2007, **259**, 432–441.
- 28 G. Bayon, S. Toucanne, C. Skonieczny, L. André, S. Bermell, S. Cheron, B. Dennielou, J. Etoubleau, N. Freslon, T. Gauchery, Y. Germain, S. J. Jorry, G. Ménot, L. Monin, E. Ponzevera, M. L. Rouget, K. Tachikawa and J. A. Barrat, *Geochim. Cosmochim. Acta*, 2015, **170**, 17–38.
- 29 D. Vance and K. Burton, *Earth Planet. Sci. Lett.*, 1999, **173**, 365–379.
- 30 J. T. Chesley, A. N. Halliday and R. C. Scrivener, *Science*, 1991, **252**, 949–951.
- 31 S. Wakaki and T. Tanaka, *Int. J. Mass Spectrom.*, 2012, **323–324**, 45–54.
- 32 A. J. McCoy-West, K. W. Burton, M.-A. Millet and P. A. Cawood, *Geochim. Cosmochim. Acta*, 2021, **293**, 575–597.
- 33 A. J. McCoy-West, M.-A. Millet and K. W. Burton, *Front. Earth Sci.*, 2020, **8**, DOI: [10.3389/feart.2020.00025](https://doi.org/10.3389/feart.2020.00025).
- 34 A. J. McCoy-West, M.-A. Millet, G. M. Nowell, O. Nebel and K. W. Burton, *J. Anal. At. Spectrom.*, 2020, **35**, 388–402.
- 35 A. J. McCoy-West, N. Mortimer, K. W. Burton, T. R. Ireland and P. A. Cawood, *Gondwana Res.*, 2022, **105**, 432–449.
- 36 A. J. McCoy-West, M.-A. Millet and K. W. Burton, *Earth Planet. Sci. Lett.*, 2017, **480**, 121–132.
- 37 X. Liu, G. J. Wei, J. Q. Zou, Y. R. Guo, J. L. Ma, X. F. Chen, Y. Liu, J. F. Chen, H. L. Li and T. Zeng, *J. Geophys. Res.: Oceans*, 2018, **123**, 9137–9155.
- 38 H. Elderfield and M. J. Greaves, *Nature*, 1982, **296**, 214–219.
- 39 J. L. Ma, G. J. Wei, Y. Liu, Z. Y. Ren, Y. G. Xu and Y. H. Yang, *J. Anal. At. Spectrom.*, 2013, **28**, 1926–1931.
- 40 N. S. Saji, D. Wielandt, C. Paton and M. Bizzarro, *J. Anal. At. Spectrom.*, 2016, **31**, 1490–1504.
- 41 C. Pin and J. F. S. Zalduegui, *Anal. Chim. Acta*, 1997, 79–89.
- 42 C. Pin, D. Briot, C. Bassin and F. Poitrasson, *Anal. Chim. Acta*, 1994, **298**, 209–217.
- 43 C. Pin and A. Gannoun, *J. Anal. At. Spectrom.*, 2019, **34**, 310–318.
- 44 C. Pin and A. Gannoun, *J. Anal. At. Spectrom.*, 2019, **34**, 2136–2146.
- 45 M. Boyet and R. W. Carlson, *Science*, 2005, **309**, 576–581.
- 46 E. Hyung and F. L. H. Tissot, *J. Anal. At. Spectrom.*, 2021, **36**, 1946–1959.
- 47 M. Rehkämper, M. Gärtner, S. J. G. Galer and S. L. Goldstein, *Chem. Geol.*, 1996, **129**, 201–208.
- 48 H. Tazoe, H. Obata and T. Gamo, *J. Anal. At. Spectrom.*, 2007, **22**, 616.
- 49 G. Caro, B. Bourdon, J.-L. Birck and S. Moorbath, *Geochim. Cosmochim. Acta*, 2006, **70**, 164–191.
- 50 P. Bonnand, C. Israel, M. Boyet, R. Doucelance and D. Auclair, *J. Anal. At. Spectrom.*, 2019, **34**, 504–516.
- 51 C.-F. Li, X.-C. Wang, Y.-L. Li, Z.-Y. Chu, J.-H. Guo and X.-H. Li, *J. Anal. At. Spectrom.*, 2015, **30**, 895–902.
- 52 Y. Wang, X. Huang, Y. Sun, S. Zhao and Y. Yue, *Anal. Methods*, 2017, **9**, 3531–3540.
- 53 Z.-Y. Chu, M.-J. Wang, C.-F. Li, Y.-H. Yang, J.-J. Xu, W. Wang and J.-H. Guo, *J. Anal. At. Spectrom.*, 2019, **34**, 2053–2060.
- 54 A. Gannoun, K. Suchorski and C. Pin, *J. Anal. At. Spectrom.*, 2022, **37**, 165–171.
- 55 J. H. Bai, F. Liu, Z. F. Zhang, J. L. Ma, L. Zhang, Y. F. Liu, S. X. Zhong and G. J. Wei, *J. Anal. At. Spectrom.*, 2021, **36**, 2695–2703.
- 56 A. Bouvier and M. Boyet, *Nature*, 2016, **537**, 399–402.
- 57 M. Garçon, M. Boyet, R. W. Carlson, M. F. Horan, D. Auclair and T. D. Mock, *Chem. Geol.*, 2018, **476**, 493–514.
- 58 L. Yang, S. Tong, L. Zhou, Z. Hu, Z. Mester and J. Meija, *J. Anal. At. Spectrom.*, 2018, **33**, 1849–1861.
- 59 J. R. de Laeter, J. K. Böhlke, P. De Bièvre, H. Hidaka, H. S. Peiser, K. J. R. Rosman and P. D. P. Taylor, *Pure Appl. Chem.*, 2003, **75**, 683–799.
- 60 T. L. Chang, Q. Y. Qian, M. T. Zhao and J. Wang, *Int. J. Mass Spectrom. Ion Processes*, 1994, **139**, 95–102.
- 61 Y. J. An, F. Wu, Y. X. Xiang, X. Y. Nan, X. Yu, J. H. Yang, H. M. Yu, L. W. Xie and F. Huang, *Chem. Geol.*, 2014, **390**, 9–21.
- 62 X. Y. Nan, F. Wu, Z. F. Zhang, Z. H. Hou, F. Huang and H. M. Yu, *J. Anal. At. Spectrom.*, 2015, **30**, 2307–2315.
- 63 G. H. Zhu, J. L. Ma, G. J. Wei and L. Zhang, *Front. Chem.*, 2020, **8**, DOI: [10.3389/fchem.2020.557489](https://doi.org/10.3389/fchem.2020.557489).
- 64 A. Pourmand and N. Dauphas, *Talanta*, 2010, **81**, 741–753.
- 65 S. Wakaki and T. Tanaka, *Int. J. Mass Spectrom.*, 2016, **407**, 22–28.
- 66 S.-A. Liu, D. Li, S. Li, F.-Z. Teng, S. Ke, Y. He and Y. Lu, *J. Anal. At. Spectrom.*, 2014, **29**, 122–133.